Lithium–Oxygen Batteries

DOI: 10.1002/anie.201102357

# The Lithium–Oxygen Battery with Ether-Based Electrolytes**

*Stefan A. Freunberger, Yuhui Chen, Nicholas E. Drewett, Laurence J. Hardwick, Fanny Bardé, and Peter G. Bruce**

The rechargeable Li–air ($O_2$) battery is receiving a great deal of interest because theoretically it can store significantly more energy than lithium ion batteries, thus potentially transforming energy storage. Since it was first described, a number of aspects of the Li–$O_2$ battery with a non-aqueous electrolyte have been investigated.[1] The electrolyte is recognized as one of the greatest challenges. To date, organic carbonate-based electrolytes (e.g. $LiPF_6$ in propylene carbonate) have been widely used.[2] However, recently, it has been shown that instead of $O_2$ being reduced in the porous cathode to form $Li_2O_2$, as desired, discharge in organic carbonate electrolytes is associated with severe electrolyte decomposition.[3] As a result it is very important to investigate other solvents in the search for a suitable electrolyte. In this regard much attention is now focused on electrolytes based on ethers (e.g. tetraglyme (tetraethylene glycol dimethyl ether)).[4] Ethers are attractive for the Li–$O_2$ battery because they are one of the few solvents that combine the following attributes: capable of operating with a lithium metal anode, stable to oxidation potentials in excess of 4.5 V versus $Li/Li^+$, safe, of low cost and, in the case of higher molecular weights, such as tetraglyme, they are of low volatility. Crucially, they are also anticipated to show greater stability towards reduced $O_2$ species compared with organic carbonates.[4]

Herein we show that although the ethers are more stable than the organic carbonates, the $Li_2O_2$ that forms on the first discharge is accompanied by electrolyte decomposition, to give a mixture of $Li_2CO_3$, $HCO_2Li$, $CH_3CO_2Li$, polyethers/esters, $CO_2$, and $H_2O$. The extent of electrolyte degradation compared with $Li_2O_2$ formation on discharge appears to increase rapidly with cycling (that is, charging and discharging), such that after only 5 cycles there is little or no evidence of $Li_2O_2$ from powder X-ray diffraction. We show that the same decomposition products occur for linear chain lengths other than tetraglyme. In the case of cyclic ethers, such as 1,3-dioxolane and 2-methyltetrahydrofuran (2-Me-THF), decomposition also occurs. For 1,3-dioxolane, decomposition forms polyethers/esters, $Li_2CO_3$, $HCO_2Li$, and $C_2H_4(OCO_2Li)_2$, and for 2-Me-THF the main products are $HCO_2Li$, $CH_3CO_2Li$; in both cases $CO_2$ and $H_2O$ evolve. The results presented herein demonstrate that ether-based electrolytes are not suitable for rechargeable Li–$O_2$ cells.

A Li–$O_2$ cell consisting of a lithium metal anode, an electrolyte, comprising 1 M $LiPF_6$ in tetraglyme, and a porous cathode (Super P/Kynar) was constructed as described in the Experimental Section. The cell was discharged in 1 atm $O_2$ to 2 V. The porous cathode was then removed, washed with $CH_3CN$, and examined by powder X-ray diffraction (PXRD) and FTIR. The results are presented in Figure 1 and Figure 2. The PXRD data demonstrate the presence of $Li_2O_2$, consistent with previous PXRD data for a Li–$O_2$ cell with a tetraglyme electrolyte at the end of the first discharge.[4a] However, examination of the FTIR spectra, Figure 2, reveals that, in addition to $Li_2O_2$, other products form. Although the FTIR spectra provide clear evidence of electrolyte decom-

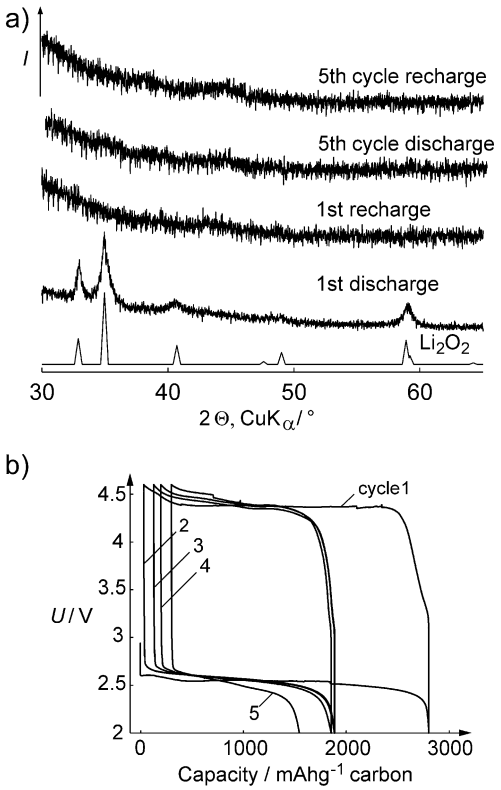


***Figure 1.*** a) Powder X-ray diffraction patterns of the composite cathode (Super P/Kynar) cycled in 1 M $LiPF_6$ in tetraglyme under 1 atm $O_2$ between 2 and 4.6 V versus $Li/Li^+$, rate = 70 $mAg^{-1}$. b) Load curves for the same cell.

[*] Dr. S. A. Freunberger, Y. Chen, N. E. Drewett, Dr. L. J. Hardwick, Dr. F. Bardé, Prof. P. G. Bruce
School of Chemistry, University of St Andrews
The Purdie Building, North Haugh
St Andrews KY16 9ST (UK)
E-mail: p.g.bruce@st-andrews.ac.uk
Dr. F. Bardé
Toyota Motor Europe, Technical Centre
Hoge Wei 33 B, 1930 Zaventem (Belgium)

[**] P.G.B. is indebted to Toyota and the EPSRC for financial support.
Supporting information for this article is available on the WWW under http://dx.doi.org/10.1002/anie.201102357.

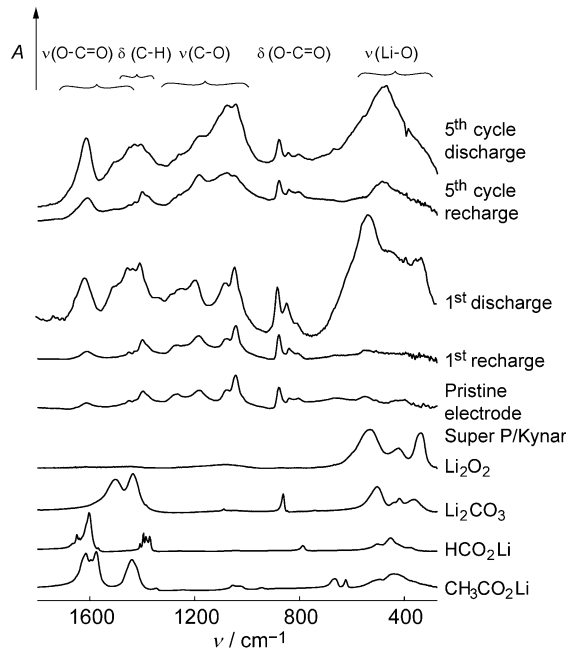


***Figure 2.*** FTIR spectra of the composite cathode (Super P/Kynar) cycled in 1 M $LiPF_6$ in tetraglyme under 1 atm $O_2$ between 2 and 4.6 V versus $Li/Li^+$. The reference spectra for $Li_2O_2$ (small peaks owing to impurity at 1080, 1450, and 1620 $cm^{-1}$), $Li_2CO_3$, $HCO_2Li$, $CH_3CO_2Li$, as well as for the pristine electrode (i.e. before cycling) are also shown. Note that the peaks in the pristine electrode arise from the Kynar.

position, it is difficult to identify all the specific discharge products by FTIR alone. To analyze the products in more detail, porous cathodes were washed with $D_2O$ and the solution then subjected to $^1H$ NMR spectroscopy (Supporting Information Figure S1). Peak assignments are listed in the Supporting Information and demonstrate the presence of $HCO_2D$ and $CH_3CO_2D$. These are consistent with the presence of $HCO_2Li$ and $CH_3CO_2Li$ in the mole ratios 1:1.2, in the porous cathode, which, on reaction with $D_2O$, form the corresponding formic and acetic acids. FTIR spectra for all the products identified in the electrode at the end of the first discharge, $Li_2O_2$ (identified from PXRD), $Li_2CO_3$ (identified from FTIR), $HCO_2Li$ and $CH_3CO_2Li$ (identified from NMR spectra) are presented in Figure 2, showing that a mixture of these compounds describes the main features of the FTIR spectrum collected from the electrode at the end of the first discharge for the tetraglyme. Mass spectrometry (MS) was carried out on the gases evolved on discharge, as described in the Experimental Section. The results show that $CO_2$ and $H_2O$ are evolved, Supporting Information Figure S2. The same MS results, showing only $CO_2$ and $H_2O$ evolution, were obtained for all the other ethers. $^1H$ NMR spectroscopy of the electrolyte at the end of discharge for this and all other cells studied, showed no evidence of any soluble discharge products.

The carbon substrate used above was Super P (61 $m^2g^{-1}$). This was replaced in turn by two other carbons of higher surface area, Ketjen Black (1400 $m^2g^{-1}$) and Black Pearls 2000 (1369 $m^2g^{-1}$). Following discharge in 1 M $LiPF_6$ in tetraglyme under 1 atm $O_2$ to 2 V, the cathodes were removed and examined by PXRD, FTIR, and NMR spectroscopy. The results are consistent with those for Super P, in that the PXRD data (Supporting Information Figure S3) show the formation of $Li_2O_2$, whereas the FTIR data (Supporting Information Figure S4) demonstrate that this species is accompanied by a number of other peaks that confirm extensive electrolyte decomposition. $^1H$ solution NMR spectroscopy after washing with $D_2O$ show the same decomposition products as in the case of Super P, although the ratios of lithium formate:lithium acetate are different and are different from each other (Ketjen Black 1:0.6, Black Pearls 1:0.8; Supporting Information Figure S1). While the main features of the FTIR spectrum for the discharged Ketjen Black electrode can be described, as for Super P, by a mixture of $Li_2O_2$, $Li_2CO_3$, $HCO_2Li$, and $CH_3CO_2Li$, all be it with different ratios (Supporting Information Figure S4) these compounds are not sufficient to explain the vibrations in the region between 1000–1300 $cm^{-1}$ in the case of Black Pearls (Supporting Information Figure S4). These bands can be assigned to polyethers/esters, that are known to have strong ν(C–O) bands in exactly this region.[5] Such compounds are anticipated based on the reaction scheme for decomposition of the ethers on discharge (Scheme 1 and Supporting Information Scheme S1). The greater presence of such species in Black Pearls, compared with the Super P and Ketjen Black (with the same surface area), may indicate a different surface chemistry for Black Pearls. We do not rule out the possibility that a small amount of polyethers/esters form on Super P and Ketjen Black at the end of discharge, but the differences between the FTIR spectra for these electrodes and the pristine electrode in the C–O region are very minor: compare the spectra at the top of Figure 2 and Supporting Information S4 with the pristine electrode in Figure 2, within the range 1100–1300 $cm^{-1}$. Overall, the nature of the electrode substrate (material) does seem to influence the discharge products to some extent.

To investigate the influence of the salt, a cell, identical to that used to collect the data in Figure 1 except that $LiPF_6$ had been replaced by LiTFSI ($LiN(SO_2CF_3)_2$), was discharged to 2 V in 1 atm $O_2$. Again the PXRD data (Supporting Information Figure S3) show $Li_2O_2$ formation. The NMR spectroscopy data are identical to those for the $LiPF_6$ salt and the FTIR data (Supporting Information Figure S4) are similar; demonstrating that changing the salt does not fundamentally change the discharge products. Cells identical to that used to collect data in Figure 1 but in which the tetraglyme is replaced by triglyme and diglyme were constructed to explore the influence of the chain length. The results are shown in the Supporting Information: Figures S1, S3 and S4. They are consistent with the tetraglyme in that only $Li_2O_2$ is apparent in the PXRD data (Supporting Information Figure S3), and the FTIR data indicate extensive electrolyte decomposition (Supporting Information Figure S4). The differences in the FTIR spectra in the region of the C–O stretching vibrations point to a greater formation of polyethers/esters in the case of the triglyme. The NMR spectroscopy results are the same for triglyme and diglyme and are very similar to those obtained for the tetraglyme. The influence of a catalyst, α-$MnO_2$ nanowires, was investigated (Supporting Information Figure S5). Although $Li_2O_2$ is present, the main discharge

  

product detected in the PXRD at the end of the 1st discharge is LiOH and FTIR reveals the presence of $HCO_2Li$, $CH_3CO_2Li$, and $Li_2CO_3$. We conclude that the extent of electrolyte decomposition is even greater with the catalyst and hence focused our studies on catalyst-free electrodes.

Although the FTIR data indicate that there are some variations between the different linear-chain ethers at the end of the first discharge, together with the PXRD and NMR data it is evident that with all such ethers the same basic products are obtained, that is, $Li_2O_2$, $Li_2CO_3$, $HCO_2Li$, $CH_3CO_2Li$, and polyether/esters. As a result, it is possible to propose a mechanistic scheme to describe the process of discharge in Li–$O_2$ cells containing such ether-based electrolytes. Scheme 1 commences with $O_2$ reduction in the cathode to $O_2^-$ [Reaction (1)] which can either react with $Li^+$ ions to

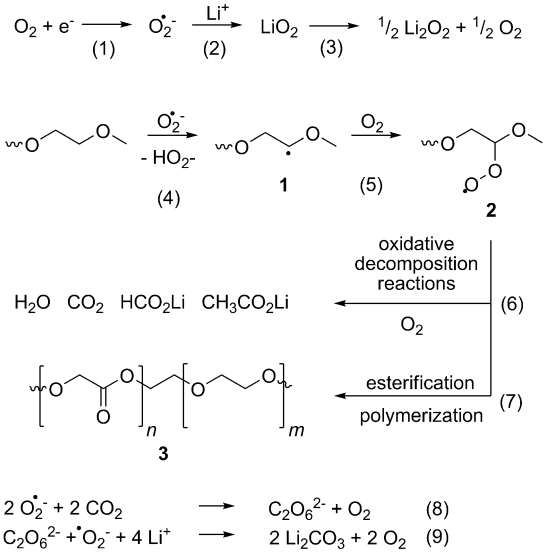


***Scheme 1.*** Proposed mechanism for reactions that occur during discharge.

form $LiO_2$ and then $Li_2O_2$ [Reactions (2) and (3)] or may abstract a proton from the glyme forming an alkyl radical that, in turn, leads to the ether peroxide **2** [Reactions (4) and (5)] (a reaction known to occur for ethers in general).[6] Species such as intermediate **2** can readily undergo oxidative decomposition reactions (analogous to combustion reactions[7]) leading to the formation of $H_2O$, $CO_2$, lithium formate, and lithium acetate [Reaction (6)] . Many oxidative decomposition pathways are possible; in modeling such reactions hundreds of pathways are often considered, which makes it virtually impossible to formulate a unique reaction path.[7] Intermediate **2** can also undergo rearrangement reactions to form the polyether/ester **3**. A more detailed pathway, expanding on Reaction (7), is given in the Supporting Information, Scheme S1. $Li_2CO_3$ can form by Reactions (8) and (9) in Scheme 1 as described previously.[8] Scheme 1 is in agreement with the widespread detection of $Li_2O_2$, $Li_2CO_3$, $HCO_2Li$, $CH_3CO_2Li$, and polyethers/esters in the PXRD, FTIR/NMR spectra. It is also in accord with mass spectrometry analysis of the gas phase at the end of discharge, which shows the presence of $H_2O$ and $CO_2$ (Supporting Information Figure S2).

Unlike the organic carbonates, the ethers do exhibit formation of $Li_2O_2$ on the first discharge. To examine what happens on charging and whether $Li_2O_2$ continues to be formed on cycling, the cell Li/1M $LiPF_6$ in tetraglyme/(Super P/Kynar) was subjected to discharge/charge cycling (Figures 1 and 2). We chose tetraglyme for the cycling studies because it has been used in Li–$O_2$ cells and is attractive for practical applications owing to its low volatility. A cell was first charged to establish the oxidation stability limit of the electrolyte, which was found to be 4.75 V (Supporting Information Figure S6; the charging limit for cell cycling was therefore set to 4.6 V). At the end of the first discharge/charge cycle the products formed on discharge appeared to have been oxidized (Figure 1 and Figure 2), only peaks corresponding to the blank electrode (the electrode before discharge) remain in the FTIR spectrum. At the end of discharge after 5 cycles, there is little or no evidence of $Li_2O_2$ in the PXRD data (Figure 1). The corresponding FTIR data show extensive electrolyte decomposition. Hence the discharge capacity of approximately 1500 $mAhg^{-1}$ on the 5th cycle arises principally from electrolyte degradation. The NMR spectroscopy data demonstrate the presence of the same products as found on the first discharge, $HCO_2Li$ and $CH_3CO_2Li$, although with significantly more $HCO_2Li$ (1:0.1). Comparing the FTIR spectra at the end of the first and fifth discharge in the region of the C–O stretch, indicates that the proportion of long-chain ethers and esters increases on cycling.

The FTIR data at the end of charging after 5 cycles demonstrate that, unlike the first cycle, a considerable quantity of the discharge products remain on charging, Figure 2. This is in agreement with the reduction in the capacity on cycling, evident in Figure 1b. We speculate that the insulating discharge products build up on the electrode surface, resulting in increasing passivation on cycling. Overall, we can conclude that although $Li_2O_2$ is formed on the first discharge the ability to do so rapidly diminishes within a few cycles, thereafter the electrochemistry is dominated by electrolyte decomposition on discharge.

Cyclic ethers, such as 1,3-dioxolane and 2-methyl-THF, have been used extensively as the basis of electrolytes in lithium batteries.[9] Each of these solvents in turn was used to replace tetraglyme in Li–$O_2$ cells, which were then discharged and subjected to analysis by PXRD, FTIR, and NMR spectroscopy. In the case of 1,3-dioxolane (Figure 3) PXRD confirms the formation of $Li_2O_2$ and FTIR shows that this is accompanied by electrolyte decomposition with bands in the C–O region suggesting ring opening and the formation of polyethers/esters and some indication of $Li_2CO_3$ and organic carbonyl species. $^1H$ solution NMR data after washing the electrode with $D_2O$ show that these organic carbonyl species are $HCO_2Li$ and $C_2H_4(OCO_2Li)_2$ in the mole ratios 1:0.4. $CH_3CO_2Li$ is detected in the NMR spectrum as a very minor quantity, less than 1% of the $HCO_2Li$. All these products are in good agreement with the reactions proposed in Supporting Information Scheme S2 for the decomposition of 1,3-dioxolane on discharge. Turning to the 2-methyl-THF, Figure 3, the

  

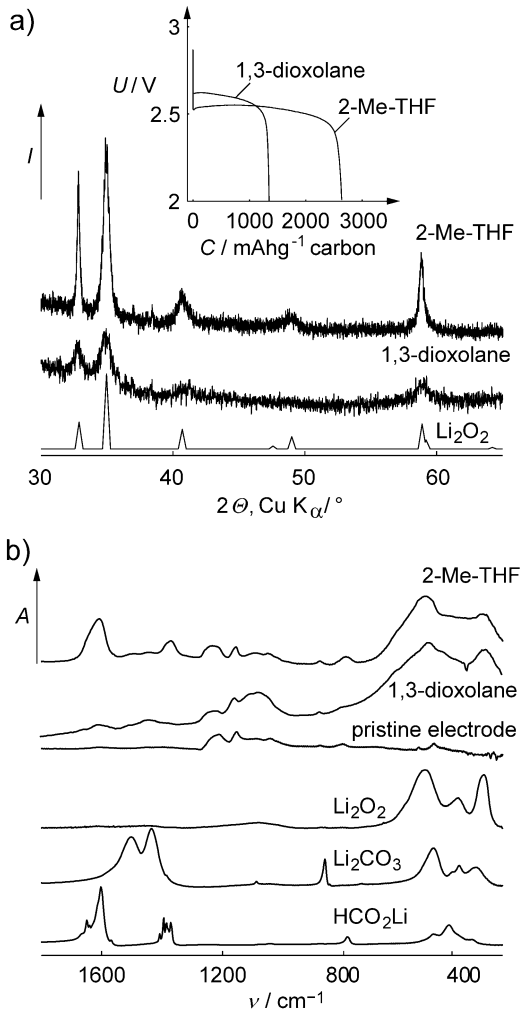


***Figure 3.*** a) Powder X-ray diffraction pattern for composite cathodes (Super P/PTFE) in either 1,3-dioxolane or 2-Me-THF, 1 M $LiPF_6$ in 1 atm $O_2$, discharged to 2 V. Inset shows the discharge curves. b) FTIR spectra of discharged composite cathodes. The reference spectra for the electrode before discharge, $Li_2O_2$, $Li_2CO_3$ and $HCO_2Li$ are also shown. Note PTFE (polytetrafluoroethylene) was used as binder instead of Kynar because the Kynar is soluble in the cyclic ethers; therefore the peaks in the pristine electrode are due to PTFE.

PXRD data indicate $Li_2O_2$ formation and the FTIR and NMR data demonstrate the presence of $HCO_2Li$ and $CH_3CO_2Li$ (1:0.3). Supporting Information Scheme S3 gives a possible reaction path for the formation of the observed discharge products.

In conclusion, by combining electrochemical measurements with powder X-ray diffraction, FTIR and NMR spectroscopy, it has been shown that electrolytes based on linear and cyclic ethers all exhibit electrolyte decomposition when used in Li–$O_2$ cells. The decomposition products for linear-chain ethers consist of a mixture of $Li_2CO_3$, $HCO_2Li$, $CH_3CO_2Li$, polyethers/esters, $CO_2$, and $H_2O$ whereas, in the case of 1,3-dioxolane, the decomposition products are polyethers/esters, $Li_2CO_3$, $HCO_2Li$, and $C_2H_4(OCO_2Li)_2$ and for 2-methyl-THF it is a mixture of $HCO_2Li$ and $CH_3CO_2Li$; $CO_2$ and $H_2O$ evolve in both cases. In all cases on the first discharge, the decomposition products are accompanied by $Li_2O_2$. However, as illustrated by cycling studies on tetraglyme (selected because it has been used in Li–$O_2$ cells and is attractive for such applications because of its low volatility) the proportion of $Li_2O_2$ diminishes on cycling in favor of greater electrolyte decomposition. Although the discharge products disappear on charging on the first cycle, they accumulate with further cycling, in accord with the reduction in the capacity with cycle number. These results lead to the conclusion that ether-based electrolytes are not suitable for Li–$O_2$ cells. Comparing ether-based electrolytes with organic carbonates, the ether-based electrolytes are more stable towards reduced $O_2$ species than the organic carbonates, as demonstrated by the formation of $Li_2O_2$ in ethers but not in organic carbonates. However, neither is stable on cycling and hence neither is suitable for Li–$O_2$ cells. Identifying solvents resistant to attack by reduced $O_2$ species remains a major challenge.

## Experimental Section

All ether solvents (Aldrich 99% +) were distilled over a packed bed column and dried for several days over freshly activated molecular sieves (type 4 Å). All solvents had a final water content of $\leq 4$ ppm (determined using a Mettler-Toledo Karl Fischer titration apparatus). Electrochemical grade $LiPF_6$ (Stella) and LiTFSI (Aldrich) were used to prepare the electrolytes. The electrochemical cells were based on a Swagelok design and comprise a Li metal anode, an electrolyte impregnated into a glass fiber separator (Whatman), and a porous cathode. The porous cathode consisted of carbon black (either Super P Li, TIMCAL, Ketjen Black EC600 JD, Akzo Nobel, or Black Pearls 2000, Cabot), Kynarflex 2801 or PTFE (mass ratio 6/4), cast on glass from a slurry made with acetone. A typical cell contained 1 mg carbon in the cathode and 0.11 g electrolyte. The cell was gastight except for the Al grid window that exposed the porous cathode to the $O_2$ atmosphere. The cell was operated in 1 atm of $O_2$. Electrochemical measurements were performed at room temperature using a Maccor battery cycler. All procedures were performed in an argon-filled glove box. Examination of electrodes involved first disassembling the cell, rinsing the cathode twice with $CH_3CN$ and removing the solvent under vacuum. Powder X-ray diffraction (PXRD) was carried out using a STOE STADI/P diffractometer operating in transmission mode with a primary beam monochromator and position sensitive detector. Cu $K_\alpha 1$ radiation ($\lambda = 1.542$ Å) was employed. The samples were contained in an airtight X-ray holder. FTIR measurements were carried out on a Nicolet 6700 spectrometer (Thermo Fisher Scientific) in transmission mode with a CsI pellet in a $N_2$ filled glove box. For $^1H$ NMR analysis the previously rinsed and dried electrodes were extracted with $D_2O$ and then the extracted solution analyzed on a Bruker Avance II 400 spectrometer. Mass spectroscopy analysis (Thermofisher) was carried out to examine the gases evolved on discharge and charge, by purging the cell with a carrier gas ($N_2$ or Ar) after charge or discharge, so that the gases evolved were transferred into the mass spectrometer.

Received: April 5, 2011
Revised: June 10, 2011
Published online: July 29, 2011

**Keywords:** electrochemistry · ethers · lithium · side reactions

[1] a) K. M. Abraham, Z. Jiang, *J. Electrochem. Soc.* **1996**, *143*, 1–5; b) J. Read, *J. Electrochem. Soc.* **2002** *149*, A1190 -A1195; c) T.

  

Ogasawara, A. Débart, M. Holzapfel, P. Novák, P. G. Bruce, *J. Am. Chem. Soc.* **2006**, *128*, 1390 – 1393; d) G. Girishkumar, B. McCloskey, A. C. Luntz, S. Swanson, W. Wilcke, *J. Phys. Chem. Lett.* **2010**, *1*, 2193 – 2203; e) T. Kuboki, T. Okuyama, T. Ohsaki, N. Takami, *J. Power Sources* **2005**, *146*, 766 – 769; f) X.-H. Yang, P. He, Y.-Y. Xia, *Electrochem. Commun.* **2009**, *11*, 1127 – 1130; g) S. D. Beattie, D. M. Manolescu, S. L. Blair, *J. Electrochem. Soc.* **2009**, *156*, A44A47; h) Y.-C. Lu, Z. Xu, H. A. Gasteiger, S. Chen, K. Hamad-Schifferli, Y. Shao-Horn, *J. Am. Chem. Soc.* **2010**, *132*, 12170 – 12171; i) G. Q. Zhang, J. P. Zheng, R. Liang, C. Zhang, B. Wang, M. Hendrickson, E. J. Plichta, *J. Electrochem. Soc.* **2010**, *157*, A953 – A956; j) J. Xiao, D. Wang, W. Xu, D. Wang, R. E. Williford, J. Liu, J.-G. Zhang, *J. Electrochem. Soc.* **2010**, *157*, A487 – A492; k) C. O. Laoire, S. Mukerjee, K. M. Abraham, E. J. Plichta, M. A. Hendrickson, *J. Phys. Chem. C* **2010**, *114*, 9178 – 9186.

[2] a) A. Débart, A. Paterson, J. Bao, P. Bruce, *Angew. Chem.* **2008**, *120*, 4597 – 4600; *Angew. Chem. Int. Ed.* **2008**, *47*, 4521 – 4524; b) S. S. Zhang, J. Read, *J. Power Sources* **2011**, *196*, 2867 – 2870; c) Y.-C. Lu, H. A. Gasteiger, M. C. Parent, V. Chiloyan, Y. Shao-Horn, *Electrochem. Solid-State Lett.* **2010**, *13*, A69 – A72; d) J.-G. Zhang, D. Wang, W. Xu, J. Xiao, R. E. Williford, *J. Power Sources* **2010**, *195*, 4332 – 4337.

[3] a) F. Mizuno, S. Nakanishi, Y. Kotani, S. Yokoishi, H. Iba, *Electrochemistry* **2010**, *78*, 403 – 405; b) S. A. Freunberger, L. J. Hardwick, Z. Peng, V. Giordani, Y. Chen, P. Maire, P. Novák, J.-M. Tarascon, P. G. Bruce, in *IMLB 2010 — The 15th International Meeting on Lithium Batteries*, Montreal, Canada, June 27 – July 2, **2010**; c) S. A. Freunberger, Y. Chen, Z. Peng, J. M. Griffin, L. J. Hardwick, F. Bardé, P. Novák, P. G. Bruce, *J. Am. Chem. Soc.* **2011** *133*, 8040 – 8047; d) W. Xu, V. V. Viswanathan, D. Wang, S. A. Towne, J. Xiao, Z. Nie, D. Hu, J.-G. Zhang, *J. Power Sources* **2011**, *196*, 3894 – 3899; e) J. Xiao, J. Hu, D. Wang, D. Hu, W. Xu, G. L. Graff, Z. Nie, J. Liu, J.-G. Zhang, *J. Power Sources* **2011**, *196*, 5674 – 5678; f) P. Albertus, G. Girishkumar, B. McCloskey, R. S. Sanchez-Carrera, B. Kozinsky, J. Christensen, A. C. Luntz, *J. Electrochem. Soc.* **2011**, *158*, A343 – A351; g) V. S. Bryantsev, M. Blanco, *J. Phys. Chem. Lett.* **2011**, 379 – 383.

[4] a) C. O. Laoire, S. Mukerjee, E. J. Plichta, M. A. Hendrickson, K. M. Abraham, *J. Electrochem. Soc.* **2011**, *158*, A302 – A308; b) J. Hassoun, F. Croce, M. Armand, B. Scrosati, *Angew. Chem.* **2011**, *123*, 3055 – 3058; *Angew. Chem. Int. Ed.* **2011**, *50*, 2999 – 3002; c) J. Read, *J. Electrochem. Soc.* **2006**, *153*, A96 – A100; d) R. A. Quinlan, Y.-C. Lu, A. N. Mansour, Y. Shao-Horn, *219th ECS Meeting — Montreal*, QC, Canada, Abstract No. 402; e) R. W. Black, S. Oh, J.-H. Lee, L. F. Nazar, *219th ECS Meeting — Montreal*, Abstract No. 426; f) B. D. McCloskey, D. S. Bethune, R. M. Shelby, G. Girishkumar, A. C. Luntz, *J. Phys. Chem. Lett.* **2011**, *2*, 1161 – 1166.

[5] a) Spectral Database for Organic Compounds SDBS, National Institute of Advanced Industrial Science and Technology; b) E. Pamula, M. Blazewicz, C. Paluszkiewicz, P. Dobrzynski, *J. Mol. Struct.* **2001**, *596*, 69 – 75.

[6] H. Rein, *Angew. Chem.* **1950**, *62*, 120.

[7] a) R. Atkinson, *Int. J. Chem. Kinet.* **1997**, *29*, 99 – 111; b) H. J. Curran, W. J. Pitz, C. K. Westbrook, P. Dagaut, J. C. Boettner, M. Cathonnet, *Int. J. Chem. Kinet.* **1998**, *30*, 229 – 241; c) O. A. Mkhatresh, F. Heatley, *Macromol. Chem. Phys.* **2002**, *203*, 2273 – 2280.

[8] a) J. L. Roberts, T. S. Calderwood, D. T. Sawyer, *J. Am. Chem. Soc.* **1984**, *106*, 4667 – 4670; b) J. D. Wadhawan, P. J. Welford, E. Maisonhaute, V. Climent, N. S. Lawrence, R. G. Compton, H. B. McPeak, C. E. W. Hahn, *J. Phys. Chem. B* **2001**, *105*, 10659 – 10668.

[9] a) D. Aurbach, Y. Gofer, *J. Electrochem. Soc.* **1991**, *138*, 3529 – 3536; b) Y. Gofer, M. Ben-Zion, D. Aurbach, *J. Power Sources* **1992**, *39*, 163 – 178.

  